Application of Digital Twin Concept in Condition Monitoring for DC-DC Converters

Yingzhou Peng
Department of energy technology
Aalborg University
Aalborg, Denmark
ype@et.aau.dk

Huai Wang
Department of energy technology
Aalborg University
Aalborg, Denmark
hwa@et.aau.dk

***Abstract*—This paper presents a digital twin-based condition monitoring method for DC-DC power converters, which features non-invasive and without additional hardware. To demonstrate it, a buck converter is applied as a case study with theoretical analysis and experimental verification. The digital twin of the buck converter is established, which includes the power stage, sampling circuit, and close-loop controller. Particle Swarm Optimization (PSO) algorithm is applied to minimize the difference between the digital twin and its physical counterpart. Compare to conventional methods, the proposed method is able to monitor the health indicators of the key components in the buck converter: capacitor and MOSFET, without adding extra measurement circuits. Moreover, because the digital twin is a replica of the physical buck converter, accessing to the internal buck converter is unnecessary, which is non-invasive.**

***Index Terms*—component, digital twin, DC-DC, health condition, parameter identification**

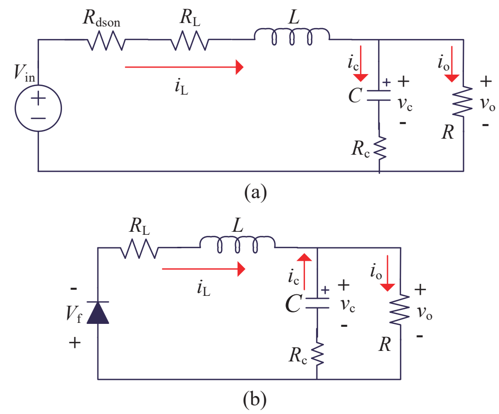

Fig. 1. Equivalent circuits of buck converter: (a)MOSFET is in on-state (b)MOSFET is in off-state.

I. Introduction

According to industry based survey [1], power semiconductor and capacitor account for more than half of the failure distribution of power converters. Thus, in order to avoid unexpected failures and leading to high maintenance cost, monitoring the health condition of these two components is meaningful.

Measurement circuit based condition monitoring methods have been proposed for measuring the health of power semiconductor switches and capacitors respectively [2] [3]. Such as the on-state resistance/voltage, threshold voltage and miller plateau in turn-on gate voltage for power semiconductor [4] [5] [6] [7]. The equivalent series resistance (ESR) and capacitance for capacitor [8] [9]. These methods are effective in monitoring the degradation of power semiconductors and capacitors. Nevertheless, additional hardware circuits are needed respectively for each component. Moreover, the failure of the added circuit may induce the failure of the component to be monitored.

To overcome the above challenges, model based parameter identification is a potential way for condition monitoring. The transfer function between the output voltage and duty cycle ratio is adopted to represent the model of DC-DC converters. Then, the coefficients of transfer function are calculated by some algorithms, such as recursive least square (RLS) in [10] and Kalman filter (KF) in [11]. This method is effective in bettering the system performance, but they are not suitable for condition monitoring. In [12], a simplified model of boost converter is built and a generalized gradient descent algorithm is used to calculate the inductance and capacitance. A model for buck converter is developed in [13], where biogeography-based optimization (BBO) method is used to identify the internal parameters. The main challenge with the above methods is that they need to access to the controller and obtain the modulation signal (duty cycle ratio) in real-time. Because only converter model is built in the above methods, whereas the sampling circuit model and controller model are not included. Moreover, all of the above methods need to inject extra signal into the controller, which is invasive to the system of interest.

In this paper, a digital twin-based condition monitoring method is proposed for DC-DC power converters. The proposed method is demonstrated by a buck converter case study. Firstly, the digital twin of buck converter including the power stage, sampling circuit, and close-loop controller is developed. This digital twin is a virtual replica of the physical buck converter system and is able to update itself continuously according to the existing measured data from its physical counterpart. Then, the particle swarm optimization (PSO) method is applied to make the difference of output waveforms between the digital twin and the physical buck converter is smaller than a pre-set threshold. Compare to conventional

978-1-7281-0395-2/19/$31.00 ©2019 IEEE

methods, the proposed condition monitoring method does not affect its physical counterpart. By data exchange with the physical system, the digital twin can update itself continuously and estimate the internal parameters of the physical system. Moreover, the proposed method does not require additional hardware and can monitor the health indicators of the key components simultaneously.

II. Digital Twin of Buck Converter

A. Buck Converter Circuit

Fig. 1 shows the equivalent circuits of Buck converter in on-state and off-state operation, which is represented by

$$\begin{bmatrix} \frac{di_L}{dt} \\ \frac{dv_c}{dt} \\ v_o \end{bmatrix} = \begin{bmatrix} -\frac{1}{L}A & -\frac{1}{L}\left(\frac{R}{R_c+R}\right) \\ \frac{1}{C}\left(\frac{R}{R_c+R}\right) & -\frac{1}{C}\left(\frac{1}{R_c+R}\right) \\ \frac{R_cR}{R_c+R} & \frac{R}{R_c+R} \end{bmatrix} \times \begin{bmatrix} i_L \\ v_c \end{bmatrix}$$
$$+D\begin{bmatrix} \frac{1}{L}V_{in} \\ 0 \end{bmatrix} + (1-D)\begin{bmatrix} -\frac{1}{L}V_f \\ 0 \end{bmatrix}$$
$$A = \left(DR_{dson} + R_L + \frac{R_cR}{R_c+R}\right) \tag{1}$$

where i_L is the inductor current, v_o is the output voltage and v_c is the capacitor voltage; R_{dson}, R_L and R_C are the parasitic resistances of MOSFET, inductor and capacitor respectively; V_{in} is the input voltage and V_f is the forward voltage of diode; D is 1 when the MOSFET is on and 0 when the MOSFET is off.

Two ways can be applied to solve (1) to obtain i_L and v_o. One is to calculate the eigenvector and eigenvalue of differential equations and construct the general solution. Then, by using the initial values of i_L and v_c, the specific solution of these differential equations can be obtained. This method demands heavy computation, especially for calculating eigenvector and eigenvalue. The other one is to linearize the differential equations with acceptable accuracy, which is used in this paper.

A typical 4^{th}-order Runge-Kutta method is used in this paper to linearize the differential equations due to the acceptable error it may cause [14]. The basic equations of 4^{th}-order Runge-Kutta are shown below:

$$y_{n+1} = y_n + \frac{h}{6}\left(k_1 + 2k_2 + 2k_3 + k_4\right) \tag{2}$$

$$\begin{aligned} k_1 &= f\left(x_n, y_n\right) \\ k_2 &= f\left(x_n + \frac{h}{2}, y_n + \frac{h}{2}k_1\right) \\ k_3 &= f\left(x_n + \frac{h}{2}, y_n + \frac{h}{2}k_2\right) \\ k_4 &= f\left(x_n + h, y_n + hk_3\right) \end{aligned} \tag{3}$$

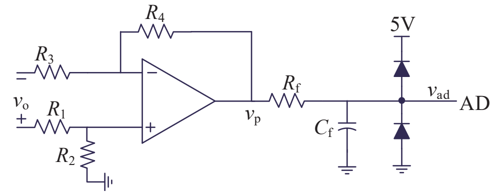

Fig. 2. Topology of sampling circuit.

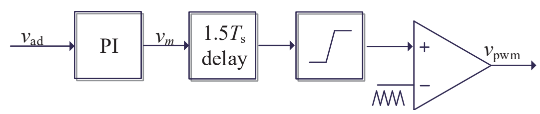

Fig. 3. Topology of close-loop controller.

where y can be either i_L or v_o, h is the calculation step time, k_1-k_4 are used to calculate the average change rate between n and $n+1$, f represents the differential equations (1). Based on (2), (1) can be transformed into linear equations. By replacing y with i_L and v_c:

$$i_{L,n+1} = i_{L,n} + \frac{h}{6}\left(k_{i1} + 2k_{i2} + 2k_{i3} + k_{i4}\right)\ (i = 1\, or\, 3) \tag{4}$$

$$v_{c,n+1} = v_{c,n} + \frac{h}{6}\left(k_{i1} + 2k_{i2} + 2k_{i3} + k_{i4}\right)\ (i = 2\, or\, 4) \tag{5}$$

$$v_{o,n+1} = i_{L,n+1}\frac{R_cR}{R_c+R} + v_{c,n+1}\frac{R}{R_c+R} \tag{6}$$

When i equals to 1 and 2, (4) represents the on-state of buck converter. When i equals to 3 and 4, (4) represents its off-state.

B. Sampling Circuit

A typical sampling circuit is adopted which includes a differential amplifier circuit and a R_fC_f low-pass filter as shown in Fig.2. The amplifier output voltage v_p is:

$$v_p = \frac{(R_3+R_4)R_2}{(R_1+R_4)R_5}v_o \tag{7}$$

The output of R_fC_f filter v_{ad} is:

$$v_{ad} = v_p - R_fC_f\frac{dv_{ad}}{dt} \tag{8}$$

According to the linearization presented by (2) and (3), (8) can be linearized as below:

$$v_{ad,n+1} = v_{ad,n} + \frac{h}{6}\left(k_1 + 2k_2 + 2k_3 + k_4\right) \tag{9}$$

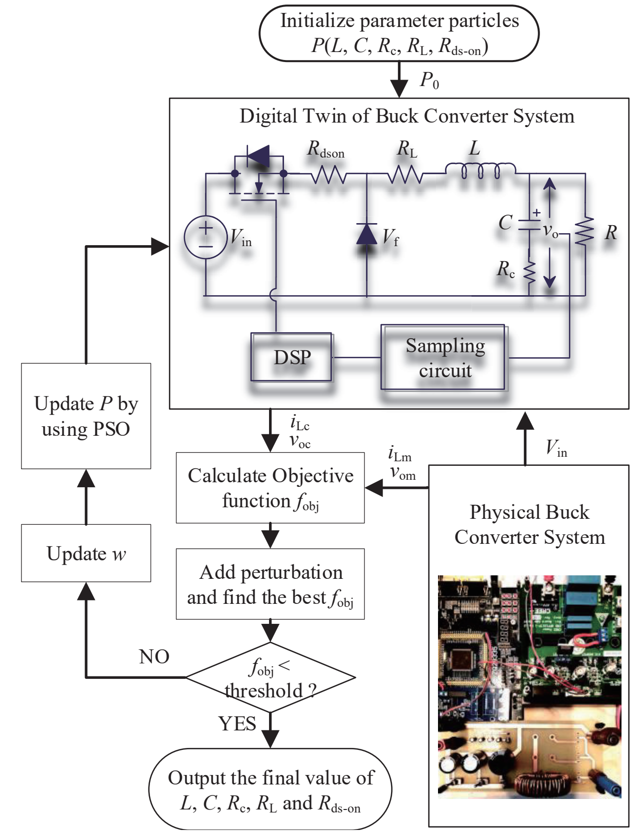

Fig. 4. Flow chat of proposed method.

C. Close-Loop Controller

To obtain modulation signal v_m, the close-loop controller is built in digital twin as shown in Fig.3. The process of controller can be expressed by the following linear equations:

$$\begin{aligned} v_{e,n} &= v_{e,n+1} \\ v_{m,n} &= v_{m,n+1} \\ v_{e,n+1} &= V_{ref} - v_{ad,n+1} \\ v_{m,n+1} &= v_{m,n} + K_p(v_{e,n+1} - v_{e,n}) + K_I h v_{e,n+1} \end{aligned} \tag{10}$$

Where V_{ref} is the reference of the output voltage, v_e is the error between the output voltage and its reference, v_m is the modulation signal, K_P and K_I are the parameters of the PI controller. Based on (10), the digital twin of buck converter can generate the modulation signal by itself instead of accessing to the physical controller. It is worth to mentioning that the sampling rate of physical buck converter system is usually set to the switching frequency and there is 1.5 times sampling period delay in updating the duty cycle ratio.

III. Application of Digital Twin with PSO

PSO is a population-based iterative optimization algorithm that mimics the swarm behavior in birds flocking and fish schooling to guide the particles to search for the global optimal solutions. Based on this, it is possible to search for the optimal solutions of the internal parameters of digital twin buck converter. To implement PSO, the first step is to construct an objective function. In this study, the objective function is:

$$f_{obj} = \frac{\sum_{i=1}^{N}\left[\left(i_{Lc,i} - i_{Lm,i}\right)^2 + \left(v_{oc,i} - v_{om,i}\right)^2\right]}{N} \tag{11}$$

where i_{Lc} and v_{oc} are the calculated inductor current and output voltage from digital twin buck converter; i_{Lm} and v_{om} are the measured data from the physical buck converter; N is the sample size of the measured data. The internal parameters of physical buck converter can be obtained by minimizing the objective function defined in (11) with PSO algorithm.

The procedure of the proposed digital twin-based condition monitoring method is shown in Fig.4. P represents the parameter set, including L, C, R_C, R_L, and R_{dson}. Firstly, the initial value of each parameter is given among a reasonable range randomly. Then, the digital twin buck converter is able to calculate the inductor current i_L and output voltage v_o. Further, the calculated i_{Lc} and v_{oc} from the digital twin buck converter and the measured i_{Lm} and v_{om} from the physical buck converter are used to calculate f_{obj} by using (11). Perturbation is then added to avoid trapping into local optima and the new best f_{obj} is found. If the f_{obj} is smaller than the pre-set threshold, the output parameter set from the digital twin represents the operational condition of physical buck converter. Otherwise, the parameter set will be updated by following equations:

$$\begin{aligned} V_{i,j} = \omega_{i-1} V_{i-1,j} &+ 2r_{1,i-1,j}\left(P_G - P_{i-1,j}\right) \\ &+ 2r_{2,i-1,j}\left(P_{L,i-1,j} - P_{i-1,j}\right) \end{aligned} \tag{12}$$

$$P_{i,j} = P_{i-1,j} + V_{i,j} \tag{13}$$

$V_{i,j}$ is the particle moving velocity of the j-th particle in i-th generation; P_G is the global optimization so far, $P_{L,i-1,j}$ is the individual optimization of the j-th particle so far; $P_{i-1,j}$ is the particle position value of the j-th particle in $(i-1)$-th generation; w is the learning factor which is updated continuously according to the method presented in [15]. r_1 and r_2 are weighting factors which are set to 2. The detail of setting learning factor and weighting factors can be referred to [15].

IV. Experimental Verifications

To validate the proposed condition monitoring method, a buck converter demonstrator is built as shown in Fig.5(a) and its specifications are presented in Table I. This study leverages the load change transients, which is relevant to many practical applications. The example waveforms are shown in Fig.5(b) and part of the waveform data are used in this study. The sampling frequency is set to 50 kHz.

By following the procedure shown in Fig.4, the internal parameters of the target buck converter can be obtained. Fig.6(a) shows the descending process of f_{obj} and its final value is 6e-4 after 50 generations. Meanwhile, these parameters converge to a stable value after 50 generations as shown in Fig.6.

TABLE I
SPECIFICATION OF BUCK CONVERTER

Specification	Value
V_{in}	24 V
V_{ref}	9 V
Switching frequency f_{sw}	20 kHz
Sampling rate f_{sr}	50 kHz
Loading 1/2	6.5 Ω / 3.7 Ω

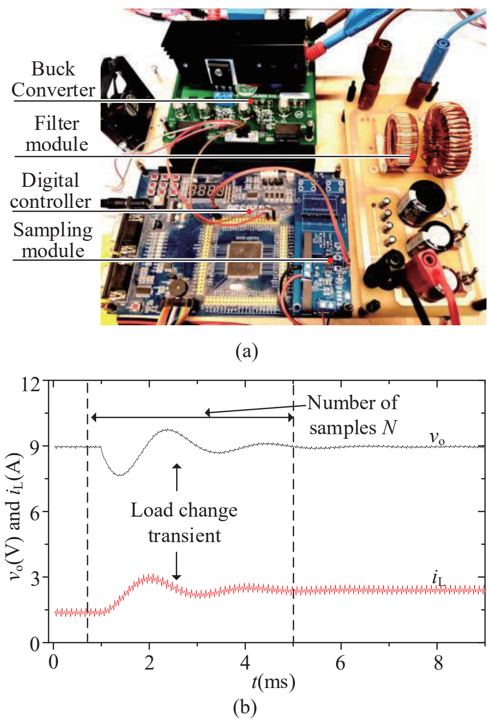

Fig. 5. Experimental demonstrator: (a) buck converter, (b) load change transient waveforms.

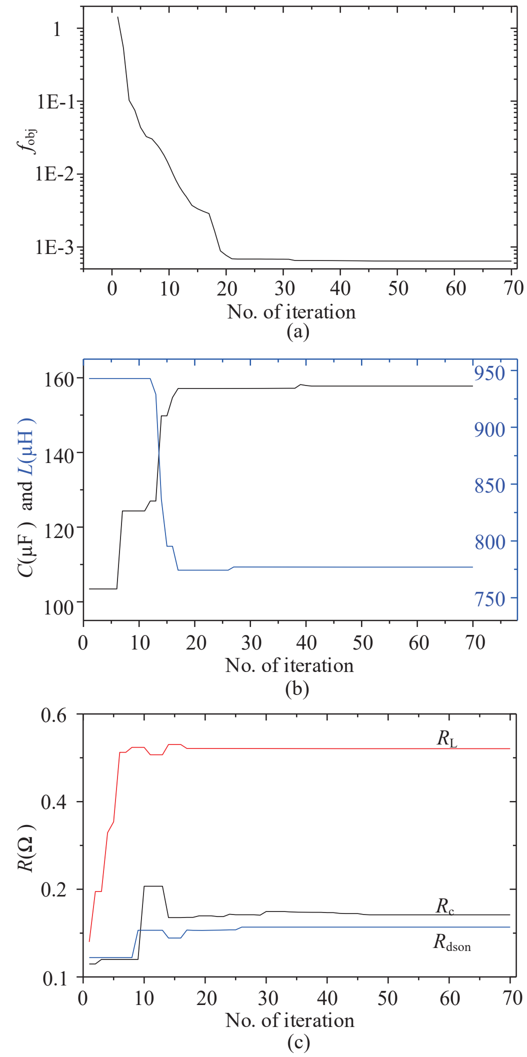

Fig. 6. Calculated results: (a) objective function, (b) inductance and capacitance, (c) parasitic resistances.

Fig.7 shows the comparative results of the estimated inductance, capacitance, and parasitic resistances and the measured ones by an LCR meter. It should be noted that the measurement conditions are under room temperature and low DC-bias voltages, being different from the conditions when the buck converter is in operation, which may result in measurement errors in itself. To investigate the consistency of the proposed method, Fig.7 includes the results from seven repeated estimations. Moreover, it can be noted that the estimated capacitance and inductance exhibit smaller errors compared to that of parasitic resistances, since the capacitor and inductor are more sensitive to the load dynamics of the buck converter.

The comparisons of i_L and v_o between the digital twin buck converter and the physical one are shown in Fig.8. It can be seen that the waveforms are very close with each other in both of static and dynamic responses.

It is still the first step towards condition monitoring by estimating the health indicators at a given condition. In practice, environmental and operation conditions can also affect the values of the health indicators, besides the degradation level of the components of interest. Moreover, as shown in Figs.7 and 8, there are certain level of estimation errors. One way to address the issue is to calibrate the components of interest at different environmental and operation conditions, as applied in [4] [16]. Nevertheless, which is time consuming and may not be practical by considering that it is necessary to calibrate each components in each produced unit due to the initial parameter variations among a population of units. In order to avoid the calibration process, this study proposes a data-cluster based method for condition monitoring method. To verify this, the proposed method is repeated for 20 times and the results of capacitance, R_L and R_{dson} are investigated.

In this study, another four capacitors with small capacitance are in parallel with the original capacitor. Then, these extra four capacitors are taken away one by one to simulate the degradation of capacitor (2.3% reduction in capacitance for removing each capacitor). Also, seven MOSFETs with different R_{dson} are used to simulate the degradation of MOSFET.

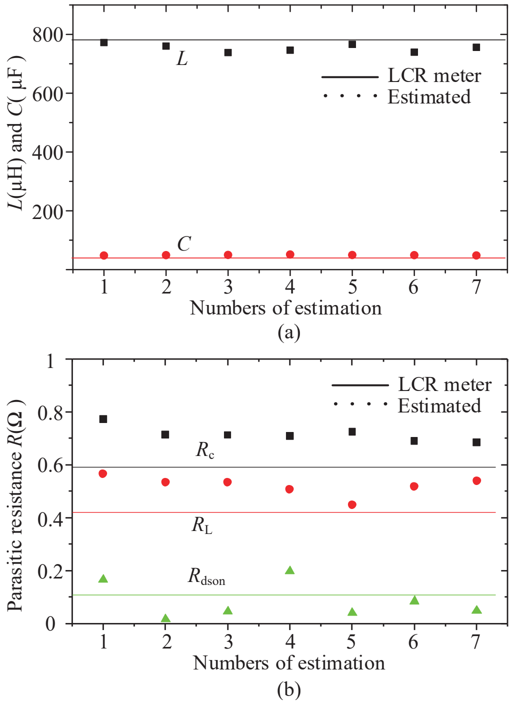

Fig. 7. Comparisons between calculated results and measured results: (a) inductance and capacitance, (b) parasitic resistances.

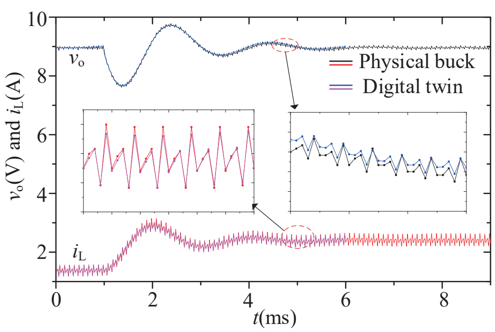

Fig. 8. Comparisons of the output waveforms between the digital twin and its physical counterpart.

Fig.9 shows the monitored capacitance descending process of capacitor. After taking away paralleled capacitors one by one, although part of the data within adjacent clusters are overlapped, collectively, the estimated data clusters are decreased constantly, which proves that the proposed method is able to monitor the degradation of capacitor in a buck converters. These estimated discrete data can not be used to indicate the health condition of capacitor directly. A further data process is needed, such as the average processing as shown in Fig.9 by the red line. More advanced algorithms can be used to do this, which is not the focus of this paper.

For MOSFET, it should be mentioned that distinguishing the R_L and R_{dson} is challenging. Because they are in series and cause same effects on the output waveforms i_L and v_o. It can be seen from Fig.10(a) and (b) that the estimated R_L and

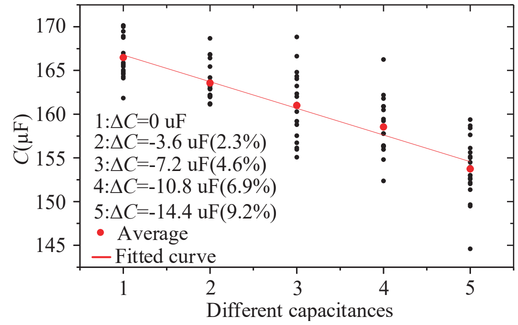

Fig. 9. Identified degradation process of capacitor.

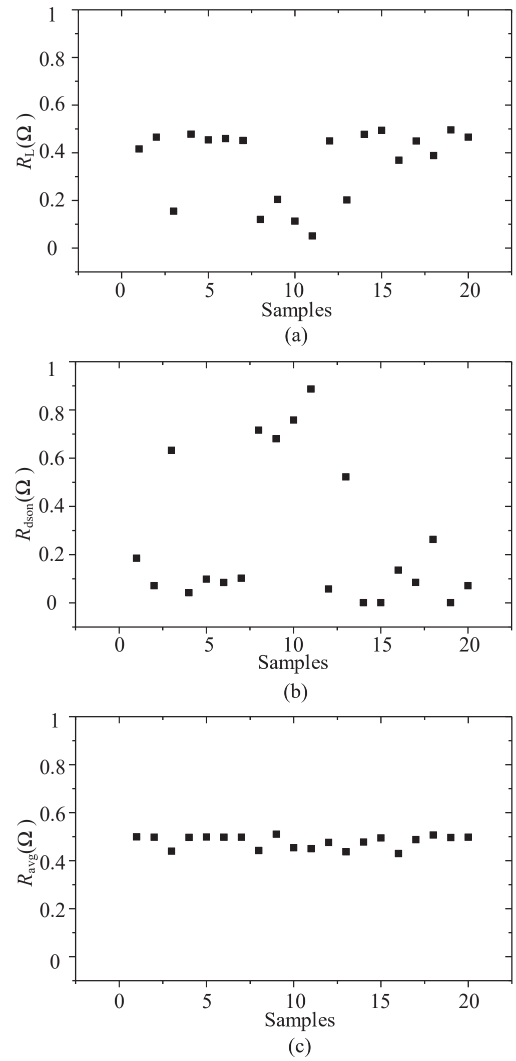

Fig. 10. Calculated parasitic resistances: (a) R_L (b) R_{dson} and (c) R_{avg}.

R_{dson} show severe uncertainty. To address this issue, a new equivalent resistance is defined in this paper to represent R_L and R_{dson}:

$$R_{avg} = R_L + DR_{dson} \tag{14}$$

D is the duty cycle ratio, which can be obtained by dividing

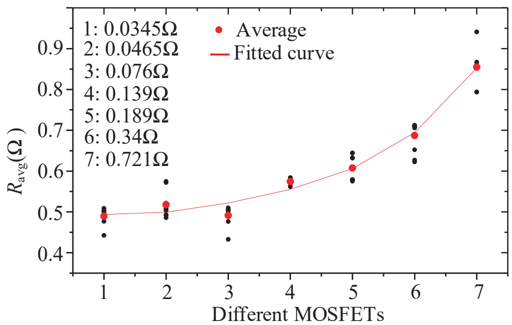

Fig. 11. Calculated R_{avg} of seven different MOSFETs with different R_{dson} (simulate the degradation process of MOSFETs).

output voltage by input voltage. By doing so, the value of R_{avg} presents much lower uncertainty as shown in Fig.10(c). Moreover, usually, the inductor has very stable characteristics and will not be aged, which enables the proposed method to monitor the change of R_{dson} via the change of R_{avg}.

The estimated R_{avg} of different MOSFET are presented in Fig,11. Similarly, the degradation process of MOSFET can be indicated by a cluster of data. According to the result shown in Fig.11, when R_{dson} is increased by 50 mΩ, the estimated R_{avg} shows identical change.

V. Conclusion

A digital twin concept based condition monitoring method is proposed for DC-DC power converters in this paper. To demonstrate this, the digital twin of buck converter is built and particle swarm optimization algorithm is applied to update the internal parameters of the digital twin by the measured data from the physical buck converter. Then both of theoretical analyses and experimental results reveal that the proposed method is able to identify the internal parameters of buck converter and make the digital twin buck converter has the similar operation waveforms with the physical one. Thereafter, the ability of monitoring the degradation of the key components (capacitor and MOSFET) is verified experimentally. Although the measurement error and inherent error could cause the fluctuation of the estimated results, it is still able to identify the degradation trend of the key components by using data-cluster based method. Compare to conventional methods, the proposed method shows non-invasive, without additional circuits and the ability of monitoring both of capacitor and MOSFET.

References

[1] S. Yang, A. Bryant, P. Mawby, D. Xiang, L. Ran, and P. Tavner, “An industry-based survey of reliability in power electronic converters,” *IEEE Transactions on Industry Applications*, vol. 47, no. 3, pp. 1441–1451, May 2011.

[2] S. Yang, D. Xiang, A. Bryant, P. Mawby, L. Ran, and P. Tavner, “Condition monitoring for device reliability in power electronic converters: A review,” *IEEE Transactions on Power Electronics*, vol. 25, no. 11, pp. 2734–2752, Nov 2010.

[3] H. Soliman, H. Wang, and F. Blaabjerg, “A review of the condition monitoring of capacitors in power electronic converters,” *IEEE Transactions on Industry Applications*, vol. 52, no. 6, pp. 4976–4989, Nov 2016.

[4] U. Choi, S. Jørgensen, and F. Blaabjerg, “Advanced accelerated power cycling test for reliability investigation of power device modules,” *IEEE Transactions on Power Electronics*, vol. 31, no. 12, pp. 8371–8386, Dec 2016.

[5] S. Dusmez and B. Akin, “An accelerated thermal aging platform to monitor fault precursor on-state resistance,” in *2015 IEEE International Electric Machines Drives Conference (IEMDC)*, May 2015, pp. 1352–1358.

[6] D. Astigarraga, F. M. Ibanez, A. Galarza, J. M. Echeverria, I. Unanue, P. Baraldi, and E. Zio, “Analysis of the results of accelerated aging tests in insulated gate bipolar transistors,” *IEEE Transactions on Power Electronics*, vol. 31, no. 11, pp. 7953–7962, Nov 2016.

[7] X. Ye, C. Chen, Y. Wang, G. Zhai, and G. J. Vachtsevanos, “Online condition monitoring of power mosfet gate oxide degradation based on miller platform voltage,” *IEEE Transactions on Power Electronics*, vol. 32, no. 6, pp. 4776–4784, June 2017.

[8] M. A. Vogelsberger, T. Wiesinger, and H. Ertl, “Life-cycle monitoring and voltage-managing unit for dc-link electrolytic capacitors in pwm converters,” *IEEE Transactions on Power Electronics*, vol. 26, no. 2, pp. 493–503, Feb 2011.

[9] N. Agarwal, M. W. Ahmad, and S. Anand, “Quasi-online technique for health monitoring of capacitor in single-phase solar inverter,” *IEEE Transactions on Power Electronics*, vol. 33, no. 6, pp. 5283–5291, June 2018.

[10] M. Algreer, M. Armstrong, and D. Giaouris, “Active online system identification of switch mode dc-dc power converter based on efficient recursive dcd-iir adaptive filter,” *IEEE Transactions on Power Electronics*, vol. 27, no. 11, pp. 4425–4435, Nov 2012.

[11] M. Ahmeid, M. Armstrong, S. Gadoue, M. Al-Greer, and P. Missailidis, “Real-time parameter estimation of dc-dc converters using a self-tuned kalman filter,” *IEEE Transactions on Power Electronics*, vol. 32, no. 7, pp. 5666–5674, July 2017.

[12] J. Poon, P. Jain, C. Spanos, S. K. Panda, and S. R. Sanders, “Fault prognosis for power electronics systems using adaptive parameter identification,” *IEEE Transactions on Industry Applications*, vol. 53, no. 3, pp. 2862–2870, May 2017.

[13] B. X. Li and K. S. Low, “Low sampling rate online parameters monitoring of dc-dc converters for predictive-maintenance using biogeography-based optimization,” *IEEE Transactions on Power Electronics*, vol. 31, no. 4, pp. 2870–2879, April 2016.

[14] J. Hult, “A fourth order runge kutta in the interaction picture method for simulating supercontinuum generation in optical fibers,” *Journal of Lightwave Technology*, vol. 25, no. 12, pp. 3770–3775, Dec 2007.

[15] Z. Zhan, J. Zhang, Y. Li, and H. S. Chung, “Adaptive particle swarm optimization,” *IEEE Transactions on Systems, Man, and Cybernetics, Part B (Cybernetics)*, vol. 39, no. 6, pp. 1362–1381, Dec 2009.

[16] S. Beczkowski, P. Ghimre, A. R. de Vega, S. Munk-Nielsen, B. Rannestad, and P. Thogersen, “Online vce measurement method for wear-out monitoring of high power igbt modules,” in *2013 15th European Conference on Power Electronics and Applications (EPE)*, Sep. 2013, pp. 1–7.